Durotropic Growth of Pollen Tubes[1][OPEN]

Ronny Reimann,[a,b,2] Delf Kah,[c,2] Christoph Mark,[c] Jan Dettmer,[a] Theresa M. Reimann,[a] Richard C. Gerum,[c] Anja Geitmann,[d] Ben Fabry,[c,3] Petra Dietrich,[b] and Benedikt Kost[a,4]

[a]Cell Biology, Department of Biology, University of Erlangen-Nuremberg, 91052 Erlangen, Germany
[b]Molecular Plant Physiology, Department of Biology, University of Erlangen-Nuremberg, 91052 Erlangen, Germany
[c]Biophysics, Department of Physics, University of Erlangen-Nuremberg, 91052 Erlangen, Germany
[d]Department of Plant Science, McGill University, Macdonald Campus, Ste-Anne-de-Bellevue, Québec H9X 3V9, Canada

ORCID IDs: 0000-0002-5492-4992 (R.R.); 0000-0002-3800-2461 (D.K.); 0000-0003-3242-6674 (T.M.R.); 0000-0003-0390-0517 (A.G.); 0000-0003-1737-0465 (B.F.); 0000-0002-9209-8089 (P.D.).

To reach the female gametophyte, growing pollen tubes must penetrate different tissues within the pistil, the female reproductive organ of a flower. Past research has identified various chemotropic cues that guide pollen tubes through the transmitting tract of the pistil, which represents the longest segment of its growth path. In addition, physical mechanisms also play a role in pollen tube guidance; however, these processes remain poorly understood. Here we show that pollen tubes from plants with solid transmitting tracts actively respond to the stiffness of the environment. We found that pollen tubes from *Nicotiana tabacum* and other plant species with a solid or semisolid transmitting tract increase their growth rate in response to an increasing matrix stiffness. By contrast, pollen tubes from *Lilium longiflorum* and other plant species with a hollow transmitting tract decrease their growth rate with increasing matrix stiffness, even though the forces needed to maintain a constant growth rate remain far below the maximum penetration force these pollen tubes are able to generate. Moreover, when confronted with a transition from a softer to a stiffer matrix, pollen tubes from *N. tabacum* display a greater ability to penetrate into a stiffer matrix compared with pollen tubes from *L. longiflorum*, even though the maximum force generated by pollen tubes from *N. tabacum* (11 μN) is smaller than the maximum force generated by pollen tubes from *L. longiflorum* (36 μN). These findings demonstrate a mechano-sensitive growth behavior, termed here durotropic growth, that is only expressed in pollen tubes from plants with a solid or semisolid transmitting tract and thus may contribute to an effective pollen tube guidance within the pistil.

Animal sperm cells have the ability to freely swim by rhythmic movements of their flagella (Malo et al., 2006). By contrast, sperm cells of angiosperm plants have lost this ability (Dresselhaus et al., 2016) and are contained within the cytoplasm of the vegetative cell of a pollen grain. Upon germination, the vegetative pollen cell forms a long tubular protrusion, the pollen tube, which rapidly elongates through the pistil and transports the enclosed immobile sperm cells toward the egg cell and the central cell for double fertilization (Zhang et al., 2017).

As opposed to cell division, pollen tubes elongate by tip growth. This process depends on a fine-tuned interplay between turgor pressure and vesicle trafficking, which delivers material required for cell wall and plasma membrane extension exclusively to the pollen tube tip (Lord, 2000; Chebli et al., 2013; Hafidh et al., 2016a; Grebnev et al., 2017; Luo et al., 2017). Therefore, only the surface at the pollen tube tip changes its relative position with respect to the environment during cell elongation, giving rise to a low-friction and thus energetically favorable growth process that has also been observed in other invasively growing cell types, such as root hairs, fungal hyphae, and neurons (Palanivelu and Preuss, 2000; Sanati Nezhad and Geitmann, 2013). This mechanism enables pollen tubes of some plant species to grow at rates of more than 300 $\mu m \cdot min^{-1}$ (Williams et al.,

[1]This work was supported by the Deutsche Forschungsgemeinschaft (DFG; grant no. RTG 1962; "Dynamic Interactions at Biological Membranes: From Single Molecules to Tissue"; grant no. TRR–SFB 225 projects A01 and C02), HHS | National Institutes of Health (NIH; grant no. HL120839), the Gouvernement du Canada | Natural Sciences and Engineering Research Council of Canada (Conseil de Recherches en Sciences Naturelles et en génie du Canada discovery grant), and Canada Research Chairs, Government of Canada (both for research from lab of A.G.).

[2]These authors contributed equally to this article.

[3]Author for contact: ben.fabry@fau.de.

[4]Senior author.

The author responsible for distribution of materials integral to the findings presented in this article in accordance with the policy described in the Instructions for Authors (www.plantphysiol.org) is: Ben Fabry (ben.fabry@fau.de).

R.R., D.K., J.D., A.G., B.F., and B.K. designed the study; R.R., C.M., and T.M.R. designed the experiments on pollen tubes growth; R.R. conducted the pollen tube experiments; R.R., D.K., C.M., and R.C.G. analyzed the experimental data; R.R., D.K., B.F., P.D., and B.K. wrote the manuscript; D.K. and B.F. designed the indenter-based experiments; D.K. conducted the indenter-based experiments; A.G. coined the term durotropism.

[OPEN]Articles can be viewed without a subscription.

www.plantphysiol.org/cgi/doi/10.1104/pp.19.01505

2016), faster than any other plant cell (Shamsudhin et al., 2016).

To reach the female gametophyte, growing pollen tubes must penetrate different tissues within the pistil. After initial growth on the surface of the stigma, pollen tubes subsequently elongate through the transmitting tract within the style and the ovary, penetrate the septum epidermis to leave the transmitting tract, continue to elongate on the surface of the funiculus and through the micropyle of the ovule, and finally enter a synergid cell, where they burst and discharge their cytoplasm together with the enclosed sperm cells (Hulskamp et al., 1995; Crawford et al., 2007). Over the past two decades, many factors have been identified that are involved in the guidance of pollen tubes along their path toward the female gametophyte, including sugars, calcium ions, nitric oxide, lipids, and secreted peptides (Hulskamp et al., 1995; Ray et al., 1997; Wolters-Arts et al., 1998; Mollet et al., 2000; Higashiyama et al., 2003; Prado et al., 2004; Chae and Lord, 2011; Sanati Nezhad et al., 2014; Qu et al., 2015; Hafidh et al., 2016b; Higashiyama and Yang, 2017; Jiao et al., 2017). Most of these chemical signals guide the pollen tubes toward and inside the ovule following their emergence from the transmitting tract. However, the transmitting tract of the pistil typically represents the longest section of the pollen tube growth path in situ (de Graaf et al., 2003; Crawford and Yanofsky, 2008). Because chemical gradients are more difficult to maintain over longer distances, physical guidance mechanisms are thought to play an important role in directing pollen tube growth within the transmitting tract (Lennon et al., 1998; Lush et al., 2000), but this has so far not been characterized in detail.

Flowers of different plant species display a highly diverse pistil and transmitting tract anatomy, which complicates the investigation of physical pollen tube guidance. Within the transmitting tract of hollow (sometimes called "open") styles, as observed for example in *Lilium longiflorum* flowers, pollen tubes grow on the epidermal surface of a cell-free canal filled with a viscous extracellular matrix (Sanders and Lord, 1992; de Graaf et al., 2001; Erbar, 2003). By contrast, the transmitting tract in solid (sometimes called "closed") styles, as found in Arabidopsis (*Arabidopsis thaliana*) and *Nicotiana tabacum* flowers, is filled with tissue composed of cells embedded in an extracellular matrix, which pollen tubes need to penetrate (Lennon et al., 1998; Cheung et al., 2000; Erbar, 2003). The tissue within the transmitting tract imposes a substantial physical resistance on pollen tube growth (Agudelo et al., 2012), in particular as intercellular spaces in this tissue are typically smaller than the pollen tube diameter (Lennon et al., 1998; Roy et al., 1999; Cheung et al., 2000).

The maximum (or stalling) force that a growing pollen tube can generate to overcome the mechanical resistance restricting its expansion within pistil tissues is determined by the product of the hydrostatic turgor pressure and the cross-sectional area of the tube at its tip. Maximum forces generated by *L. longiflorum* tubes measured with capacitive force sensors (Burri et al., 2018) were found to be in the range of 9.6 ± 1.6 μN, whereas forces generated by *Camellia japonica* pollen tubes measured with soft microcantilevers (Ghanbari et al., 2018) were found to be around 1.5 μN. However, direct force measurements using capacitive force sensors or microcantilevers are technically highly demanding (Agudelo et al., 2013; Ghanbari et al., 2014; Sanati Nezhad et al., 2014). Moreover, measurements of the maximum stalling force cannot provide information on the penetration force of a pollen tube growing inside a pistil under physiological conditions, as this force depends on the growth rate and the mechanical impedance of the surrounding matrix (Sanati Nezhad et al., 2013).

In this study, we present a method to estimate the penetration force generated by a pollen tube tip during its growth through matrices of different stiffness. With this method, we investigated pollen tubes from plant species, both with hollow and with solid styles, and measured the relationship between penetration force and growth rate for matrices with different mechanical properties. We found that pollen tubes from plants with solid styles, but not those from plants with hollow styles, increase their growth rate in matrices with higher physical resistance, indicating that an active mechanosensory mechanism controls the tropic growth of these pollen tubes, which may help them to navigate through the complex architecture of the pistil to reach the female gametophyte. We propose the term *durotropism* for this mechanosensory mechanism that guides pollen tubes from plants with solid styles toward stiffer environments, analogous to the term *durotaxis* that describes the preferential migration of mammalian mesenchymal cells toward regions with higher substrate rigidity (Lo et al., 2000).

RESULTS

Penetration Force Measurements during Pollen Tube Growth

Physical guidance implies that the pollen tube probes and actively or passively responds to the mechanical properties of the environment. Such mechanoresponsiveness requires that the pollen tube applies forces to the environment. During growth, pollen tubes generate forces that are equal and opposite to the resisting forces of the matrix. For growth through a viscous matrix, these forces, according to Stoke's law, equal the product of tip radius, growth rate, matrix viscosity, and a shape factor of 3π for the hemispherical shape of the moving tip. Thus, to estimate the penetration force of a pollen tube, it is sufficient to know the matrix viscosity and to measure tip radius and growth rate from microscopic time-lapse images.

For growth through an elastic matrix, the situation is more complicated, as penetration forces also depend on

the matrix stiffness and hence the density of chemical bonds between the matrix molecules, their rupture energy, the propagation behavior of cracks that form at the front of the advancing pollen tube tip, and a large number of other factors. Moreover, penetration forces can no longer be expected to increase linearly with growth rate or tip radius.

In the following, we investigated pollen tube growth through an elastic agarose-solidified pollen tube culture medium, which we used here as a substitute for the tissue of the transmitting tract. To alter the mechanical stiffness of the matrix, we adjusted the agarose concentrations between 0.1% and 3%. To estimate the forces generated during pollen tube growth through differently concentrated agarose gels, we measured the forces needed to advance steel needles with a hemispherical tip and diameters ranging from 100 to 700 μm at penetration speeds between 200 μm/min and 5 mm/min (Fig. 1A). We then applied a scaling relationship to scale down these forces to the size and velocity of pollen tubes. We found that the force needed to penetrate agarose gels increases in proportion with the needle diameter d to the power of 2, the penetration velocity v to the power of 0.2, and the agarose concentration $c_{agarose}$ to the power of 1.79:

$$F = F_0 \cdot d^2 \cdot v^{0.2} \cdot c_{agarose}^{1.79} \quad (1)$$

The pre-factor F_0 is $7.29 \cdot 10^{-4}$ μN when d is given in units of micrometers, $c_{agarose}$ is given in percent (w/v) agarose, and v is given in units of micrometers per minute. With this simple empirical relationship, the penetration forces of pollen tubes growing through an elastic matrix can be computed from the tip diameter and growth rate as measured from microscopic time-lapse images. For a typical *N. tabacum* pollen tube with a diameter of 11 μm growing at a speed of 5 μm/min (Geitmann et al., 1996), Equation 1 predicts a force of 0.12 μN in 1% agarose, 0.42 μN in 2% agarose, and 0.87 μN in 3% agarose. Given that maximum stalling forces of pollen tubes have been reported to be around 10 μN (Supplemental Table S1), Equation 1 predicts that the growth rate of pollen tubes falls below 5 μm/min in a ≥12% agarose gel. Thus, by measuring the retardation of pollen tube

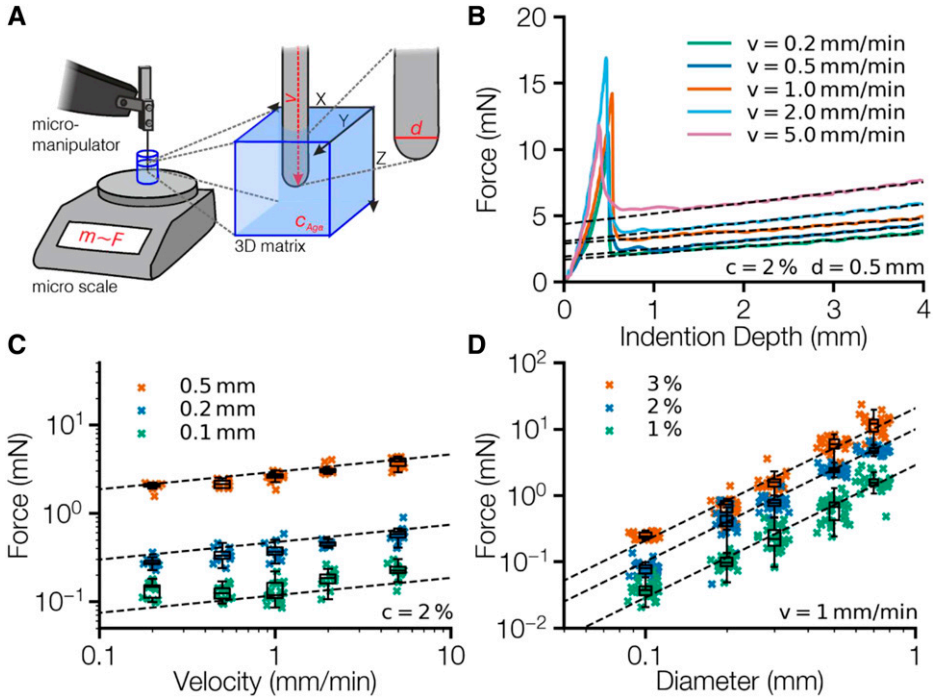

Figure 1. Estimating pollen tube forces. A, Experimental setup: a cylindrical steel needle with a hemispherical tip was driven with a defined velocity into an agarose gel. The indentation force was monitored with a standard laboratory precision scale. B, Exemplary force measurements for a 0.5-mm diameter needle driven into 2% agarose gels at different velocities. After the gel surface was punctured, the indentation forces rose linearly with indentation depth due to increased surface friction. This friction, which does not occur in a growing pollen tube, can be canceled by performing a linear fit (dashed lines) between 2 to 4 mm depth and by extrapolating the indentation force to zero depth. C, The indentation force at zero depth depends on both the needle diameter and velocity. Symbols show data from individual measurements, boxes show mean and quartiles, whiskers the 5 and 95 percentiles without outliers. Dashed lines are the predictions from Equation 1. D, Indentation forces at zero depth for different needle diameters and agarose concentrations. Symbols show data from individual measurements, boxes show mean and quartiles, whiskers show the 5 and 95 percentiles without outliers. Dashed lines are the predictions from Equation 1.

growth under conditions of high matrix stiffness, we can estimate a lower boundary for the maximum force that a pollen tube can generate.

Maximum Force Estimation

To estimate the maximum penetration force (F_{max}) that can be generated by growing pollen tubes, *N. tabacum* or *L. longiflorum* pollen grains were germinated in a pipette tip filled with 1% agarose that was inserted into a 12% agarose gel. We investigated only those tubes that grew toward the 12% agarose gel (Fig. 2A). We prevented a sharp boundary between the two gels by thermal annealing that lead to the formation of an interphase region with a smooth stiffness gradient, as confirmed by the diffusion of 0.5-μm fluorescent beads from the 1% gel into the 12% gel (Fig. 2A; Supplemental Fig. S1). We considered the gel region into which no beads had diffused as a pure 12% agarose gel and started the measurements only once the pollen tubes had reached this region.

Pollen tubes from both species were able to grow beyond the interphase region into the 12% agarose matrix, but they adjusted their growth rates differently. The growth rate of pollen tubes from *N. tabacum* steadily slowed down from ~5 μm/min to below 0.5 μm/min in the 12% agarose matrix, whereas the tip diameter steadily increased from 10 to 18 μm (Fig. 2B). The resulting forces remained approximately constant during this process and reached 10.9 μN on average (Fig. 2, B and D). By contrast, pollen tubes from *L. longiflorum* did not slow down during the observation period, whereas the tip diameter fluctuated around a value of 22 μm and the forces fluctuated around 36.1 μN on average (Fig. 2, C and D). Because the growth rate remained substantially above zero in the 12% matrix, this value represents a lower boundary for F_{max}. By dividing the force with the cross-sectional area of the tube at its tip, the corresponding penetration pressure was 51.4 ± 3.4 kPa for *N. tabacum* and 113.1 ± 8.5 kPa for *L. longiflorum* (Fig. 2E).

Force-Velocity Relationship during Pollen Tube Growth

Intuition predicts that the rate of pollen tube growth increases with lower agarose concentration (and hence lower resisting forces) up to a maximum rate that is limited by the ability to incorporate new material into the cell wall of the growing tip. To measure the force versus growth rate relationship over a large range of matrix stiffnesses, pollen tubes were grown in medium solidified with agarose at concentrations between 0.1% and 3% (Table 1). A maximum agarose concentration of 3% was used, because at higher concentrations the medium became too viscous, preventing the uniform dispersion of pollen grains at a temperature of 37°C, which could not be exceeded without adverse effects on pollen vitality.

To investigate if the force versus growth rate relationship depends on the in situ environment in which pollen tubes normally grow, we analyzed pollen tubes from species displaying three distinct types of transmitting tract anatomy and stiffness (Fig. 3A; Supplemental Fig. S2): (1) Arabidopsis, *N. tabacum*, bonnet pepper

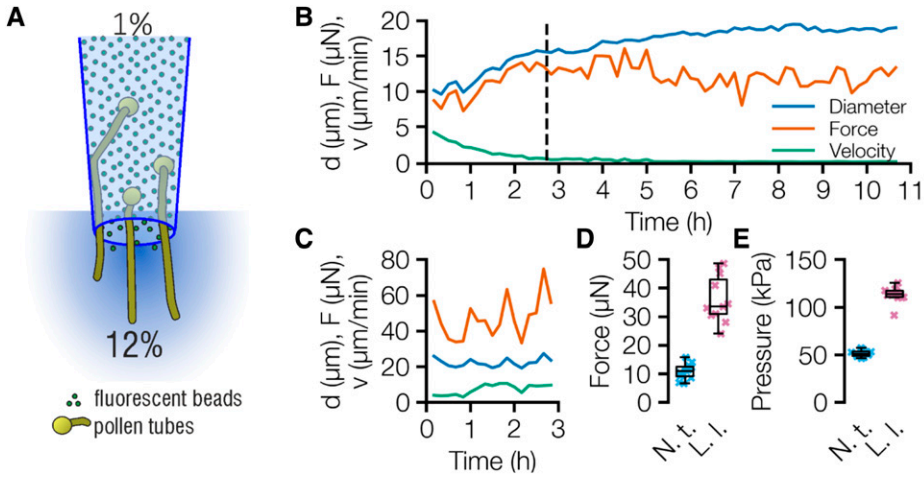

Figure 2. Maximum forces generated by *N. tabacum* and *L. longiflorum* pollen tubes. A, Experimental setup: Pollen grains were germinated in a soft 1% agarose gel inside a pipette tip, and emerging tubes grew toward and into a stiff 12% agarose gel. B and C, Time evolution of pollen tube diameter, growth velocity, and force of exemplary pollen tubes growing in 12% agarose. Whereas pollen tubes of *N. tabacum* (B) decreased their growth rate as they grew into the stiffer medium, they simultaneously increased in diameter, resulting in a nearly constant force. By contrast, pollen tubes of *L. longiflorum* (C) showed fluctuating diameters, growth rates, and forces. D, Mean penetration forces were 10.9 ± 2.8 μN for *N. tabacum* (n = 12, evaluated at a growth rate of 0.5 μm/min as indicated by the dashed line in [B]) and 36.1 ± 8.2 μN for *L. longiflorum* (n = 11). E, Effective penetration pressures (force divided by cross-sectional area at the tip base) were 51.4 ± 3.4 kPa for *N. tabacum* and 113.1 ± 8.5 kPa for *L. longiflorum*.

Table 1. *Pollen tube culture media*

–, zero/no substance was added.

Substance	Arabidopsis	*L. longiflorum, C. chinense, C. trachelium*	*E. californica*	*N. tabacum, H. fulva, S. chacoense*
$CaCl_2*2H_2O$	2.00 mM	0.20 mM	–	1.00 mM
$Ca(NO_3)_2*4H_2O$	2.00 mM	1.29 mM	1.52 mM	1.00 mM
$MgSO_4*7H_2O$	1.00 mM	–	1.65 mM	1.00 mM
KNO_3	–	1.0 mM	1.00 mM	–
KCl	1.00 mM	–	–	–
H_3BO_3	1.62 mM	0.16 mM	1.62 mM	1.62 mM
Suc	18% (w/v)	10% (w/v)	10% (w/v)	10% (w/v) for *N.t.* and *H.f.*, 12% (w/v) for *S.c.*
pH	7.0	7.0–7.5	6.8–7.0	7.5
Reference	Bou Daher et al., 2009	Li et al., 1996	Kakani et al., 2002	Brewbaker and Kwack, 1963

(*Capsicum chinense*), and a wild potato (*Solanum chacoense*), which are all members of the nightshade family and grow flowers with a solid transmitting tract; (2) the nettle-leaved bellflower (*Campanula trachelium*), the Easter lily (*L. longiflorum*), and the orange day-lily (*Hemerocallis fulva*), which grow flowers with a hollow style covered with a viscous extracellular matrix (Sanders and Lord, 1989); and (3) the California poppy (*Eschscholzia californica*), which grows flowers with long stigmatic protrusions and a hollow style covered with papilla and papilla-like cells, respectively, below which pollen tubes are growing (Becker et al., 2005). This anatomy is referred to as semisolid in the following.

Starting point for the growth rate analysis was 20 min after germination (*S. chacoense* 10 min) to ensure all pollen tubes had already entered a phase of relatively uniform growth. For averaging, a time window of 60 min (*S. chacoense* 30 min) was chosen in order to not exclude the fastest pollen tubes from the analysis, which over longer time periods would grow out of the microscope's field of view.

Under all conditions and for pollen tubes from all plant species, average growth rates were above 1 μm/min (Fig. 3B), and the resulting forces were below 2 μN (Fig. 3C). Pollen tubes from plants with a hollow style grew fastest, with speeds exceeding 5 μm/min under all conditions (Fig. 3B, right), whereas pollen from plants with semisolid or solid transmitting tract grew considerably slower, with speeds below 5 μm/min (Fig. 3B, left).

Pollen tubes normally growing in hollow styles slowed down by 30% as the resisting forces increased by more than 10-fold at higher agarose concentrations (Fig. 3B, right; Fig. 3C; Supplemental Table S2). This observation is in line with the notion that growth rate in the low-force regime is predominantly limited by the speed with which new material can be incorporated into the cell wall of the growing tip. By contrast, pollen tubes from flowers with solid styles did not slow down with higher matrix resistance but, unexpectedly, even increased their growth rate with higher agarose concentrations (Fig. 3B, left). This speeding up could reach up to 50%, whereas the resisting forces increased by more than 10-fold (Fig. 3C; Supplemental Table S2). We are not aware of a passive mechanism in any living system that increases the speed of motility or growth in response to increasing resisting forces, and thus we conclude that the observed speeding up of pollen tube growth is due to an active mechanoresponsive, durotropic growth process. Note that this speeding up is eventually limited by the maximum force that the pollen tube can generate; hence, *N. tabacum* pollen tubes stall rather than display further speeding up in a 12% agarose matrix compared with a 3% matrix (Fig. 2B).

To test if the growth-promoting effect of a stiffer matrix is in fact caused by the resistance of the matrix and not by a chemical agarose component, *N. tabacum* pollen tubes were grown on the surface of medium solidified with 1% or 3% agarose rather than inside the medium. Possible chemical effects should still be able to influence pollen tube growth, whereas the effect of matrix resistance is excluded in this setting. We found no differences in growth rate at different agarose concentrations (Supplemental Fig. S3) and can therefore exclude a dose-dependent effect of a chemical agarose component. Instead, we argue that the observed increase of growth rate at higher agarose concentrations was due to physical effects.

Pollen Tube Growth across Interfaces between Gels with Different Stiffness

Since an increase of growth rate with increasing matrix stiffness is only observed for pollen tubes that are normally growing in a solid or semisolid style, we speculate that the underlying mechanism might be an adaptive mechanism that helps the pollen tube to navigate more efficiently through the complex tissue of the transmitting tract. To test if pollen tubes from plants with different style architectures show differences in their physical guiding behavior, we observed their growth at the interface between agarose gels of different stiffness (Fig. 4, A and B). For this, we prepared gels with agarose concentrations of 1%, 2%, 3%, 4%, 5%, or 6% in a mold with 5-mm cubic-shaped openings (Supplemental Fig. S4) that were filled with medium containing 1% or 3% agarose, in which pollen grains from *N. tabacum* or *L. longiflorum* were evenly distributed

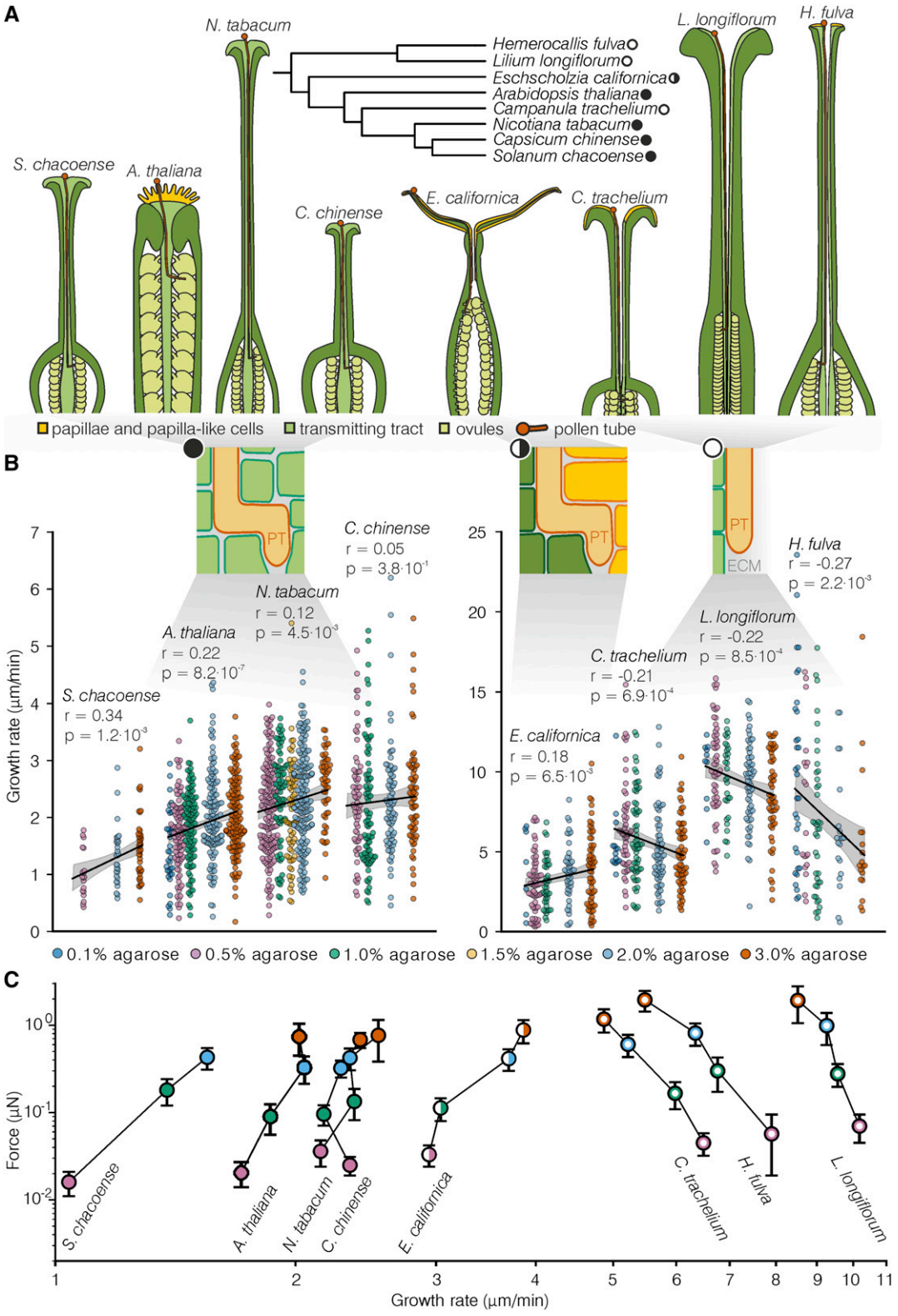

Figure 3. Pistil structure and dependence of pollen tube growth rate on the mechanical resistance of the medium. A, Pistil structure and transmitting tract anatomy of investigated plant species. The pollen tube growth path is indicated in dark orange. Enlarged sections illustrate pollen tubes growing within tissues or the extracellular matrix of the transmitting tract. Drawings are not to scale. Empty circles. hollow transmitting tract filled with a viscous extracellular matrix (ECM); half-filled circle. semisolid transmitting tract where stigmatic protrusions are lined with an epidermal layer of papillae and papilla-like cells (yellow); filled

and germinated. This inner gel is subsequently referred to as the starting phase, and the surrounding gel is referred to as the target phase. For each pollen tube that reached the interface between the two phases, the approach angle at the interface and the crossing success (yes/no) were recorded. For each condition, we computed the probability that the pollen tube crosses the interface as a function of the approach angle (Eq. 2).

As expected, we found the highest crossing success for an approach angle of 90°, regardless of plant species and agarose concentrations of the starting or target phase. Furthermore, the crossing success tended toward zero for small approach angles (Fig. 4C) and for higher agarose concentrations of the target phase (Figs. 4, D and E). The crossing success was considerably lower than 100% for a 90° approach angle also in situations with an equal starting phase/target phase combination (1%/1% or 3%/3%; Fig. 4, D and E). We hypothesize that the microscopic structure of the agarose polymer at the interface hinders the spreading of material cracks in front of the advancing pollen tube, and that the build-up of force needed to form a new crack across the interface (similar to the initial force build-up seen in Fig. 1B) leads to a turn in the growth direction of the pollen tube. This hypothesis is supported by the observation that the crossing success was higher for a 1%/1% compared with a 3%/3% starting phase/target phase combination.

Interestingly, we found marked differences in the behavior between the two plant species. For *L. longiflorum* (hollow style), the crossing success into both a soft (1%) and intermediate (2%) target phase was considerably higher when growing from a stiffer (3%) starting phase compared with the crossing success when growing from a softer (1%) starting phase, as one would expect for a pollen tube that passively responds to the stiffness gradient (Fig. 4D). By contrast, for *N. tabacum* (solid style), the crossing success into both a soft (1%) and intermediate (2%) target phase was considerably higher when growing from the softer (1%) starting phase compared with the crossing success when growing from a stiffer (3%) starting phase (Fig. 4E). This finding demonstrates a preference of pollen tubes from *N. tabacum* for growing in a stiffer matrix and is in line with our finding of an increased growth rate in stiffer matrices. This preference is further underscored by the observation that *N. tabacum* pollen tubes could grow from a 1% gel into a 4% or 5% gel, whereas *L. longiflorum* pollen tubes could not.

DISCUSSION

Pollen Tube Growth and Invasive Force in a Three-Dimensional Matrix

In this study, we present a method for estimating the penetration force of pollen tubes growing in an agarose matrix. According to an empirical scaling relationship (Eq. 1), this force can be calculated from the agarose concentration, tip diameter, and growth rate, which scale with power law exponents of 1.79, 2, and 0.2, respectively.

The power-law exponents for concentration and growth rate were obtained from a global fit of penetration force measurements using blunt needles with hemispherical tips and different diameters that were driven at a range of speeds through gels with variable agarose concentrations. The power-law exponent of 1.79 for the force-dependence on agarose concentration agrees with published data showing that the stiffness of 0.1% to 2% agarose gels scales with concentration to the power of 1.7 under compression and 1.8 under tension (Normand et al., 2000). The exponent of 0.2 for the growth rate indicates that agarose, like other hydrogels, displays pronounced non-Newtonian plastic flow behavior (when sheared beyond the yield stress), whereby the shear stress increases with strain rate (velocity) to a power smaller than unity. However, we are not aware of published values for the power-law velocity exponent of solidified agarose under plastic flow conditions.

The power-law exponent of 2 for the tip diameter was chosen based on the assumption that the number of agarose bonds that a growing tip needs to break during the growth process scales with the cross-sectional area of the pollen tube. When we included the tip diameter exponent as a free fit parameter, we obtained a value of 1.79. However, the quality of the global fit improved only marginally whereas the uncertainty of the other two fit parameters increased noticeably.

Because we extrapolated the penetration forces of 10 to 20 μm thick pollen tubes from measurements of 100 to 700 μm thick steel needles, the relative uncertainty of our force estimation is 19%, as determined by bootstrapping. Moreover, we could only estimate a lower bound for the maximum force, because our method

Figure 3. (*Continued.*)
circles. solid transmitting tract. Inset. phylogenetic tree of the investigated plant species. B, Growth rate of *S. chacoense*, Arabidopsis, *N. tabacum*, *C. chinense*, *E. californica*, *L. longiflorum*, *C. trachelium*, and *H. fulva* pollen tubes. Each point corresponds to the velocity of an individual pollen tube averaged over 60 min (30 min *S. chacoense*), starting 20 min (10 min for *S. chacoense*) after germination. Agarose matrix concentrations are indicated by different colors. The black line shows the linear trend of growth rate in relation to the agarose concentration; gray shaded area indicates the confidence interval of the linear trend. The Pearson correlation coefficient and its *P*-value are listed above each line. C, Growth rates and corresponding penetration forces (mean ± SD) estimated from Equation 1 using values for pollen tube diameters determined in separate experiments under the same conditions.

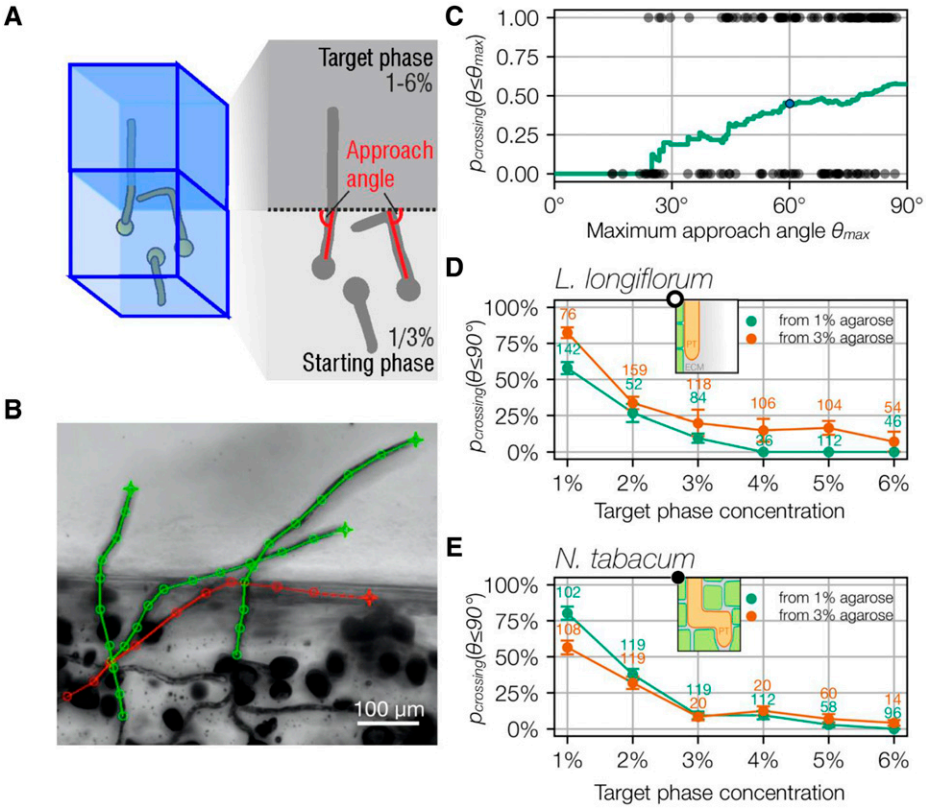

Figure 4. Pollen tube growth across interfaces between gels of different stiffness. A, Schematic of the experimental setup. Pollen grains were germinated in 1% or 3% agarose medium (starting phase) and grew toward a 1%, 2%, 3%, 4%, 5%, or 6% agarose medium (target phase). The approach angle θ is the angle between the interface plane and the average growth direction inside the starting phase for the last 50 min before reaching the interface. B, Exemplary bright field minimum projection image showing *N. tabacum* pollen tubes growing from a 1% agarose starting phase into a 1% agarose target phase. Each marker point represents the position of the pollen tube tip in consecutive frames of an image series taken at 10-min intervals. Of the four pollen tubes that reached the interface, the one with the smallest approach angle (red) was not able to grow into the target phase but instead continued to grow along the interface. C, Probability of interface crossing ($p_{crossing}(\theta \leq \theta_{max})$) for *L. longiflorum* pollen tubes with approach angles $\theta \leq \theta_{max}$ from a 1% agarose starting phase into a 1% agarose target phase. For example (blue data point), $p_{crossing}(\theta \leq 60^{\circ})$ was 45% for pollen tubes with an approach angle of 60° or smaller. D, $p_{crossing}(\theta \leq 90^{\circ})$ of *L. longiflorum* pollen tubes (hollow transmitting tract) for all combinations of starting and target phases. Data points indicate mean ± SE of as many pollen tubes as indicated by the numbers above each data point. E, $p_{crossing}(\theta \leq 90^{\circ})$ of *N. tabacum* pollen tubes (solid transmitting tract) for all combinations of starting and target phases. Data points indicate mean ± SE of as many pollen tubes as indicated by the numbers above each data point.

requires that the pollen tube is still able to grow. Nonetheless, the maximum penetration forces measured with our method (11 μN for *N. tabacum* and 36 μN for *L. longiflorum*) are in the same range as stalling forces measured with capacitive force sensors (29 μN for *L. longiflorum*; Burri et al., 2018).

By dividing the maximum force by the cross-sectional area of the pollen tube at its tip base, we determined a lower bound for the driving pressure P_{max} of 51.4 ± 3.4 kPa for *N. tabacum* and 113.1 ± 8.5 kPa for *L. longiflorum*. The latter value is at the lower end of the turgor pressure range of 100 to 400 kPa as measured in growing pollen tubes of *L. longiflorum* (Benkert et al., 1997), indicating that the cell wall represents a barrier to the internal pressure and reduces the pressure that can be exerted onto an outside substrate. Indeed, published evidence demonstrates that when faced with an obstacle, pollen tubes do not increase turgor pressure but reduce cell wall stiffness at the apex (Fayant et al., 2010), which is also in line with our finding of increased tube diameters and tube bursting when approaching the stalling force (Fig. 2B; Supplemental Fig. S1).

Durotropic Growth of Pollen Tube

The main finding of this study is the discovery of an active response of pollen tube growth to the mechanical resistance of the surrounding matrix by which growth in mechanically stiffer environments is promoted. Moreover, our data show that this durotropism is displayed only by pollen tubes from plant species with a

solid style. Our findings are consistent with previous anecdotal reports that pollen tubes from Arabidopsis (solid style) prefer an agarose-stiffened medium compared with a liquid medium, whereas pollen tubes from *Papaver rhoeas* (common poppy, hollow style) prefer a softer substrate (Gossot and Geitmann, 2007; Ghanbari et al., 2018). The preference of pollen tubes from solid-style species for stiffer medium raises the question of the guidance mechanism that makes these pollen tubes leave the septum and transmitting tract to grow on the surface of the funiculus and ovule, an environment that does not pose substantial mechanical resistance. It appears that in this situation the local chemical guidance cues attracting pollen tubes toward receptive ovules may dominate over any mechanical preferences.

The observation that phylogenetically remotely related plant species (Fig. 3A, inset) can display similar style architectures and similar behavior of pollen tube growth suggests that the expression or activation of durotropism depends foremost on style architecture, regardless of the phylogenetic background. In addition to the general tendency of pollen tubes from plants with a solid style to speed up in stiffer matrices and pollen from plants with a hollow style to slow down, we also observed marked differences in the average growth rates of pollen tubes from different species. In particular, we found that pollen tubes from plants with hollow styles grew faster compared with pollen tubes from plants with solid styles. This finding is in line with previous reports of evolutionary adaptation so that the in situ pollen tube pathway length is correlated to the pollen tube growth rate and that angiosperms with longer styles have, in general, faster pollen tube growth rates (Williams, 2012). In our choice of investigated plant species, hollow-style plants tend to have longer styles, hence their higher growth rate.

We furthermore noted that pollen tubes from hollow-style plant species included in this study also tended to have larger diameters and consequently grew with higher penetration forces at all investigated agarose concentrations (Fig. 3C). For example, the maximum penetration force of pollen tubes from *L. longiflorum* (hollow style) was at least four times higher compared with the maximum force of *N. tabacum* (solid style). As a consequence, pollen tubes from *L. longiflorum*, even though they prefer to grow in softer matrices, were able to grow also in very stiff matrices (12% agarose gels) in which pollen tubes from *N. tabacum*, even though they prefer to grow in stiffer matrices, slowed down, stopped, and finally burst. Thus, relative growth rate in response to matrix stiffness, absolute growth rate, and maximum force are independent parameters and are differently correlated with style properties.

Previous studies have measured a force threshold at which pollen tubes change their growth behavior, whereby the tubes grow straight and unhindered into a capacitive force sensor. At a force threshold of 3.0 μN for Arabidopsis and 9.6 μN for *L. longiflorum*, the pollen tubes stalled and then changed growth direction (Burri et al., 2018). Our data show changes in the pollen tube growth rate at much lower forces of 0.016 μN for Arabidopsis and 0.070 μN for *L. longiflorum* (Supplemental Table S2). Such low forces, however, cannot be measured with capacitive force sensors or soft cantilevers, and thus we argue that our method, due to its sensitivity in particular for very small forces, provides a suitable approach to establish a perceptive force threshold.

Finally, we found that differences in the mechanoresponsiveness of pollen tube growth rates correlate with differences in the guiding behavior during growth. At smooth interfaces between two matrices, pollen tubes from *N. tabacum* (solid style) crossed from a stiffer (3%) into a softer (1%) agarose matrix with a lower probability compared with the crossing between two equal (1%) interfaces, suggesting that they prefer to grow on the stiffer side. By contrast, pollen tubes from *L. longiflorum* (hollow style) crossed from a stiffer (3%) into a softer (1%) agarose matrix with a higher probability compared with the crossing between two equal (1%) interfaces, suggesting that they prefer to grow on the softer side. We also observed that the success rate for crossing an interface strongly depended on the approach angle, even for interfaces between matrices with the same stiffness (Fig. 4A). Thus, guiding behavior that confers a tendency to remain in the current environment could be observed for pollen tubes from plants with either solid or hollow styles.

CONCLUSION

Our data demonstrate a durotropic behavior of pollen tube growth that is only expressed by pollen tubes from plants with a solid or semisolid transmitting tract. Pollen tubes from these plants increase their growth rate with increasing matrix stiffness, whereas pollen tubes from plant species with a hollow transmitting tract decrease their growth rate. At the interface between environments of different stiffness, *N. tabacum* pollen tubes (solid style) prefer to grow on the stiffer side, whereas *L. longiflorum* pollen tubes (hollow style) prefer to grow on the softer side. Thus, the mechanoresponse of pollen tube growth is adapted to the physical environment provided by the style and appears to contribute to an effective pollen tube guidance required for fertilization.

MATERIALS AND METHODS

Microindentation

Microindentation experiments were conducted using an InjectMan NI 2 micromanipulator (Eppendorf AG) with a custom-built holder for attaching indenter needles. Acupuncture needles with 0.1-, 0.2-, and 0.3-mm diameters (Seirin Corporation), as well as 0.5- and 0.7-mm diameters (wandrey GmbH) were used as indenters. To match the geometry of a pollen tube, the needle tips were manually sanded to a hemispherical shape. Previously prepared agarose gels (fabricated with *Nicotiana tabacum* culture medium) were thawed at 65°C for 20 min, following which a volume 250 μL was carefully (to avoid air bubbles) pipetted into wells from 96-well break-out microplates (Nalge Nunc

International) and allowed to solidify for 20 min at room temperature. The wells were then filled to the top with DPBS (Dulbecco's phosphate-buffered saline; Life Technologies) to prevent evaporation. Without this liquid layer, agarose gels showed increasing stiffness within 30 min after solidification (data not shown). With a liquid layer, however, no gel stiffening was found within 2 h after solidification (data not shown). Weight changes during indentation were recorded with a laboratory scale equipped with an RS232 interface (Practum 64-1S, Sartorius) and converted to forces.

Penetration Force as a Function of Indentation Speed and Indenter Diameter

The indenter tip (for needle diameters of 0.1, 0.2, and 0.5 mm) was first moved manually into the liquid layer above the agarose layer (agarose concentration of 2% [w/v]) and then lowered with a speed of 20 μm/s toward the agarose surface, which was reached when the measured weight exceeded a threshold of 5 μg. From this point onward, the agarose gel was indented to a depth of 4 mm at constant speeds of 0.2, 0.5, 1, 2, or 5 mm/min. The weight and indentation depth were continuously measured at a rate of 5 Hz. The indentation force was obtained by multiplying the measured weights with the gravitational constant.

We found that the force increased strongly with indentation depth for the first ~500 to 1000 μm and fell abruptly once the indenter tip had punctured the agarose surface (Fig. 1B). After this point, the penetration force increased slowly and linearly with indentation depth. The slope of the force depended linearly on indentation speed and needle diameter due to friction. To estimate the indentation force in the absence of friction, we performed a linear fit of the measured force versus indentation curve for indentation depths between 2 to 4 mm and extrapolated to the point of zero indentation depth (dashed line in Fig. 1B). We repeated measurements ($n = 10$) for each combination of needle diameter and indentation speed.

We then fitted the measured forces to an expression of the form $Force = a \cdot diameter^2 \cdot velocity^b$ (diameter in units of micrometer, velocity in units of micrometer per minute) by minimizing the squared error of the logarithm of the measured and fitted force values (Fig. 1C). Fitting was performed using the *curve_fit* function of the *SciPy* package in *python*. We found an excellent fit (correlation $R^2 = 0.98$) with fit parameters $a = 2.98 \cdot 10^{-3} \mu N, b = 0.20$.

Penetration Force as a Function of Agarose Concentration

We repeated indentation experiments for different agarose concentrations (1%, 2%, and 3% [w/v]) and needle diameters (0.1, 0.2, 0.3, 0.5, and 0.7 mm) with a constant indentation speed of 1 mm/min ($n \geq 25$ repeats for every combination). We then fitted the measured forces to an expression of the form $Force = F_0 \cdot diameter^2 \cdot velocity^{0.2} \cdot conc_{agarose}^{c}$ (Fig. 1D; diameter in units of micrometer, velocity in units of micrometer per minute, concentration in units of percent [w/v] agarose) and obtain values of $F_0 = 7.29 \cdot 10^{-4} \mu N$ and $c = 1.79$, with a correlation between fitted and measured forces of $R^2 = 0.93$.

Penetration Force as a Function of the Culture Medium

To test whether different culture media that are used for the preparation of the agarose gels and as a top layer during indentation experiments influence the mechanical properties of agarose, we performed an additional set of indentation experiments (Supplemental Fig. S5). We tested 1% (w/v) agarose gels that were fabricated and topped-up with the four different culture media used for pollen tube experiments (see section *Pollen tube growth conditions* and Table 1). For each condition, we performed 15 indentation measurements with a fixed needle diameter (0.3 mm) and indentation speed (1 mm/min). The median indentation forces of agarose prepared with *N. tabacum*, *Lilium longiflorum*, and *Eschscholzia califonica* medium were nearly identical and also in close agreement with the value obtained for an agarose gel prepared with *N. tabacum* medium and a DPBS top layer (220 μN, Fig. 1D). However, the indentation force for agarose gels prepared with Arabidopsis (*Arabidopsis thaliana*) culture medium that contained higher concentrations of Ca^{2+} and Suc were 29% higher compared with the other conditions. Accordingly, we used a calibration constant of $F_0 = 9.42 \cdot 10^{-4} \mu N$ for computing the penetration forces of Arabidopsis pollen tubes.

Cultivation of Plants

Arabidopsis ecotype Col-0 and *N. tabacum* 'Petit Havana SR1' plants were cultivated at 22°C, 60% relative humidity under long-day conditions (16-h light, 8-h dark). Unopened flowers of *L. longiflorum* were obtained from a local florist and kept at room temperature (22°C to 25°C) until the anthers were mature. All other plants were cultivated in a greenhouse: *Eschscholzia californica* at 16°C and *Capsicum chinense* and *Solanum chacoense* at 22°C. *Campanula trachelium* and *Hemerocallis fulva* were collected from a garden near Erlangen.

Pollen Tube Growth Conditions

Pollen tubes of *N. tabacum*, *H. fulva*, and *S. chacoense* were grown in Brewbaker-Kwak medium (Brewbaker and Kwack, 1963). Pollen tubes of Arabidopsis and *E. californica* were grown in modified B Brewbaker-Kwak medium (Table 1; Kakani et al., 2002; Bou Daher et al., 2009). Pollen tubes of *C. chinense*, *L. longiflorum*, and *C. trachelium* were grown in medium optimized for *Lilium* as described in Li et al. (1996; compare with Table 1). All pollen tubes were grown at room temperature (22°C). Pollen tube media were mixed with different concentrations of low-melting agarose (CAS no. 39346-81-1, Carl Roth GmbH + Co. KG), boiled once, and stored at −20°C. Aliquots were liquefied at 75°C for 20 to 25 min and then cooled down to 37°C before usage. Flowers of the different species were hydrated in a box with moist wipes for at least 1 h before pollen grains were harvested by shaking out the anthers or by briefly vortexing the flowers in medium. Pollen grains were suspended in 100 to 200 μL of liquid medium without agarose, and aliquots (10–20 μL) were then evenly resuspended in 2 to 5 mL of 37°C medium with different agarose concentrations. The resulting suspensions of pollen grains and agarose-containing medium were then quickly filled in the culture vessels and solidified at room temperature (22°C) for 15 min.

Analysis of Pollen Tube Growth in a Three-Dimensional Matrix

To measure the growth of pollen tubes, a light microscope equipped with a 10× 0.25 NA (5× 0.12 NA for *L. longiflorum* and *H. fulva*) objective, a 0.5× video coupler, and a motorized microscope stage were used to record bright-field image stacks (z-distance 10 μm) at 10-min intervals (2.5 min for *S. chacoense*) over a total duration of 1 to 12 h depending on pollen tube growth. From the image stacks, we computed and stored minimum intensity projections and, separately for each pixel, the z-position where the minimum intensity was found. Pollen tube growth trajectories (x,y positions only) were tracked from the minimum intensity projection images using the image annotation software ClickPoints (Gerum et al., 2017). For each pollen tube growth trajectory, the mean growth velocity was computed from a linear fit to the data. We ignored the z-component of the growth velocity because of the low accuracy (±10 μm) with which we could determine the z-position of the tip from the z-stack images. Our value under-estimates the true growth velocity by a factor of $\sin\theta$, where θ is the polar angle of the growth direction with the z-direction. On average, $\sin\theta$ was 0.8 in our dataset; thus, we systematically underestimate the magnitude of the growth velocity by 20% and the penetration force by 4.4%.

Diameter Analysis

The diameter of pollen tubes was measured at the base of the tip from bright field images using the image annotation software ClickPoints (Gerum et al., 2017).

Force and Pressure

The forces at the pollen tube tip during growth were estimated from the tip diameter and the growth rate with Equation 1. For estimating the pressure, we divided the force by the cross-sectional area of the pollen tube at the base of the tip.

Maximum Force Measurements

To estimate the F_{max}, pollen grains were germinated in medium with 1% (w/v) agarose in a cutoff pipette tip. The opening of the tip was then lowered into a 12% (w/v) agarose gel heated to 95°C (Fig. 2A). The high temperature of the 12% agarose medium leads to a partial melting of the solidified inner 1% gel. This approach avoided a sudden concentration and stiffness boundary between the two different gels and instead lead to the formation of an interphase region with a smooth stiffness gradient, as confirmed by the diffusion of 0.5-μm

fluorescent beads from the 1% gel into the 12% gel (Fig. 1A; Supplemental Fig. S1). We analyzed only pollen tubes that grew toward the 12% gel and that remained in focus during the entire observation period (i.e. they showed only small movements in z-direction). Images were taken every 10 min. The evaluated pollen tubes of *N. tabacum* grew on average 578 ± 89 μm (mean ± SD, n = 12) into the 12% gel before coming to a stop. They were observed for an average duration of 407 ± 90 min. Pollen tubes of *L. longiflorum* grew into the 12% gel without reducing the speed until they left the field of view after a distance of 1313 ± 385 μm (mean ± SD, n = 11). They were observed for an average duration of 208 ± 65 min. All tubes from both species grew beyond the bead-containing interphase region well into the 12% gel region during the observation period.

Pollen Tube Growth at Stiffness Interfaces

To generate a layered gel structure with two different agarose concentrations and a planar boundary between the two layers, we placed four quadratic plastic pillars (LEGO bricks) with a cross section of 5 × 5 mm into each well of a 6-well plate. Then 5 mL of pollen tube growth medium containing 1%, 2%, 3%, 4%, 5%, or 6% (w/v) agarose was then added to each well and kept at 4°C for 10 min to allow for solidification. The plastic pillars were then carefully removed, and the resulting holes were filled with pollen grains dispersed in growth medium containing 1% or 3% agarose. After solidification, images of growing pollen tubes were obtained as described above. Pollen tubes that had reached the interface were manually tracked using the image annotation software ClickPoints (Gerum et al., 2017). From the growth direction during the last 50 min before reaching the interface, we determined the approach angle θ between the pollen tube and the planar interface. Additionally, we recorded for each pollen tube that had reached the interface whether it succeeded in crossing the interface. We computed the crossing probability of all recorded pollen tubes up to a maximum approach angle θ_{max} according to

$$p_{crossing}(\theta \le \theta_{max}) = \frac{n_+(\theta \le \theta_{max})}{n_-(\theta \le \theta_{max}) + n_+(\theta \le \theta_{max})} \quad (2)$$

where $n_+(\theta \le \theta_{max})$ is the number of successful crossing attempts for pollen tubes with a crossing angle of θ_{max} or smaller, and $n_-(\theta \le \theta_{max})$ is the respective number of unsuccessful crossing attempts.

Supplemental Data

The following supplemental materials are available.

Supplemental Figure S1. Pollen tube growth in 12% agarose gels for maximum force estimation.

Supplemental Figure S2. Style architecture of the investigated plant species.

Supplemental Figure S3. Test for potential secondary effects from low-melting agarose on pollen tube growth.

Supplemental Figure S4. Method for producing interfaces with agarose compartments of different stiffness.

Supplemental Figure S5. Indentation forces in agarose gels with different media compositions.

Supplemental Table S1. Overview Force-Measurements in growing pollen tubes.

Supplemental Table S2. Overview of pollen tube diameter, growth velocities, and forces exerted by pollen tubes of different species when growing through matrices of different stiffness.

ACKNOWLEDGMENTS

We thank Olli Torvinen for help with indentation and pollen tube diameter measurements, Valentin Joly for help with pollen tube growth experiments, and Hana Rakusová and Youssef Chebli for helpful discussions.

Received January 28, 2020; accepted March 23, 2020; published April 2, 2020.

LITERATURE CITED

Agudelo CG, Sanati Nezhad A, Ghanbari M, Naghavi M, Packirisamy M, Geitmann A (2013) TipChip: A modular, MEMS-based platform for experimentation and phenotyping of tip-growing cells. Plant J **73:** 1057–1068

Agudelo CG, Sanati A, Ghanbari M, Packirisamy M, Geitmann A (2012) A microfluidic platform for the investigation of elongation growth in pollen tubes. J Micromech Microeng **22:** 115009

Becker A, Gleissberg S, Smyth DR (2005) Floral and vegetative, orphogenesis in california poppy (*Eschscholzia californica* cham.). Int J Plant Sci **166:** 537–555

Benkert R, Obermeyer G, Bentrup F-W (1997) The turgor pressure of growing lily pollen tubes. Protoplasma **198:** 1–8

Bou Daher F, Chebli Y, Geitmann A (2009) Optimization of conditions for germination of cold-stored Arabidopsis thaliana pollen. Plant Cell Rep **28:** 347–357

Brewbaker JL, Kwack BH (1963) The essential role of calcium ion in pollen germination and pollen tube growth. Am J Bot **50:** 859–865

Burri JT, Vogler H, Läubli NF, Hu C, Grossniklaus U, Nelson BJ (2018) Feeling the force: How pollen tubes deal with obstacles. New Phytol **220:** 187–195

Chae K, Lord EM (2011) Pollen tube growth and guidance: Roles of small, secreted proteins. Ann Bot **108:** 627–636

Chebli Y, Kroeger J, Geitmann A (2013) Transport logistics in pollen tubes. Mol Plant **6:** 1037–1052

Cheung AY, Wu H-M, di Stilio V, Glaven R, Chen C, Wong E, Ogdahl J, Estavillo A (2000) Pollen-pistil interactions in *Nicotiana tabacum*. Ann Bot (Lond) **85:** 29–37

Crawford BC, Ditta G, Yanofsky MF (2007) The NTT gene is required for transmitting-tract development in carpels of Arabidopsis thaliana. Curr Biol **17:** 1101–1108

Crawford BC, Yanofsky MF (2008) The formation and function of the female reproductive tract in flowering plants. Curr Biol **18:** R972–R978

de Graaf BH, Knuiman BA, Derksen J, Mariani C (2003) Characterization and localization of the transmitting tissue-specific PELPIII proteins of *Nicotiana tabacum*. J Exp Bot **54:** 55–63

de Graaf BHJ, Derksen JWM, Mariani C (2001) Pollen and pistil in the progamic phase. Sex Plant Reprod **14:** 41–55

Dresselhaus T, Sprunck S, Wessel GM (2016) Fertilization mechanisms in flowering plants. Curr Biol **26:** R125–R139

Erbar C (2003) Pollen tube transmitting tissue: Place of competition of male gametophytes. Int J Plant Sci **164:** S265–S277

Fayant P, Girlanda O, Chebli Y, Aubin CE, Villemure I, Geitmann A (2010) Finite element model of polar growth in pollen tubes. Plant Cell **22:** 2579–2593

Geitmann A, Li YQ, Cresti M (1996) The role of the cytoskeleton and dictyosome activity in the pulsatory growth of *Nicotiana tabacum* and *Petunia hybrida* pollen tubes. Bot Acta **109:** 102–109

Gerum RC, Richter S, Fabry B, Zitterbart DP (2017) ClickPoints: An expandable toolbox for scientific image annotation and analysis. Methods Ecol Evol **8:** 750–756

Ghanbari M, Nezhad AS, Agudelo CG, Packirisamy M, Geitmann A (2014) Microfluidic positioning of pollen grains in lab-on-a-chip for single cell analysis. J Biosci Bioeng **117:** 504–511

Ghanbari M, Packirisamy M, Geitmann A (2018) Measuring the growth force of invasive plant cells using Flexure integrated Lab-on-a-Chip (FiLoC). Technology (Singap) **6:** 101–109

Gossot O, Geitmann A (2007) Pollen tube growth: Coping with mechanical obstacles involves the cytoskeleton. Planta **226:** 405–416

Grebnev G, Ntefidou M, Kost B (2017) Secretion and endocytosis in pollen tubes: Models of tip growth in the spot light. Front Plant Sci **8:** 154

Hafidh S, Fíla J, Honys D (2016a) Male gametophyte development and function in angiosperms: A general concept. Plant Reprod **29:** 31–51

Hafidh S, Potěšil D, Fíla J, Čapková V, Zdráhal Z, Honys D (2016b) Quantitative proteomics of the tobacco pollen tube secretome identifies novel pollen tube guidance proteins important for fertilization. Genome Biol **17:** 81

Higashiyama T, Kuroiwa H, Kuroiwa T (2003) Pollen-tube guidance: Beacons from the female gametophyte. Curr Opin Plant Biol **6:** 36–41

Higashiyama T, Yang WC (2017) Gametophytic pollen tube guidance: Attractant peptides, gametic controls, and receptors. Plant Physiol **173:** 112–121

Hulskamp M, Schneitz K, Pruitt RE (1995) Genetic evidence for a long-range activity that directs pollen tube guidance in Arabidopsis. Plant Cell **7:** 57–64

Jiao J, Mizukami AG, Sankaranarayanan S, Yamguchi J, Itami K, Higashiyawma T (2017) Structure-activity relation of AMOR sugar molecule that activates pollen-tubes for ovular guidance. Plant Physiol **173:** 354–363

Kakani VG, Prasad PVV, Craufurd PQ, Wheeler TR (2002) Response of in vitro pollen germination and pollen tube growth of groundnut (*Arachis hypogaea* L.) genotypes to temperature. Plant Cell Environ **25:** 1651–1661

Lennon KA, Roy S, Hepler PK, Lord EM (1998) The structure of the transmitting tissue of *Arabidopsis thaliana* (L.) and the path of pollen tube growth. Sex Plant Reprod **11:** 49–59

Li Y-Q, Zhang H-Q, Pierson ES, Huang F-Y, Linskens HF, Hepler PK, Cresti M (1996) Enforced growth-rate fluctuation causes pectin ring formation in the cell wall of *Lilium longiflorum* pollen tubes. Planta **200:** 41–49

Lo CM, Wang HB, Dembo M, Wang YL (2000) Cell movement is guided by the rigidity of the substrate. Biophys J **79:** 144–152

Lord E (2000) Adhesion and cell movement during pollination: Cherchez la femme. Trends Plant Sci **5:** 368–373

Luo N, Yan A, Liu G, Guo J, Rong D, Kanaoka MM, Xiao Z, Xu G, Higashiyama T, Cui X, et al (2017) Exocytosis-coordinated mechanisms for tip growth underlie pollen tube growth guidance. Nat Commun **8:** 1687

Lush WM, Spurck T, Joosten R (2000) Pollen tube guidance by the pistil of a solanaceous plant. Ann Bot (Lond) **85:** 39–47

Malo AF, Gomendio M, Garde J, Lang-Lenton B, Soler AJ, Roldan ERS (2006) Sperm design and sperm function. Biol Lett **2:** 246–249

Mollet J-C, Park S-Y, Nothnagel EA, Lord EM (2000) A lily stylar pectin is necessary for pollen tube adhesion to an in vitro stylar matrix. Plant Cell **12:** 1737–1750

Normand V, Lootens DL, Amici E, Plucknett KP, Aymard P (2000) New insight into agarose gel mechanical properties. Biomacromolecules **1:** 730–738

Palanivelu R, Preuss D (2000) Pollen tube targeting and axon guidance: Parallels in tip growth mechanisms. Trends Cell Biol **10:** 517–524

Prado AM, Porterfield DM, Feijó JA (2004) Nitric oxide is involved in growth regulation and re-orientation of pollen tubes. Development **131:** 2707–2714

Qu LJ, Li L, Lan Z, Dresselhaus T (2015) Peptide signalling during the pollen tube journey and double fertilization. J Exp Bot **66:** 5139–5150

Ray SM, Park SS, Ray A (1997) Pollen tube guidance by the female gametophyte. Development **124:** 2489–2498

Roy SJ, Holdaway-Clarke TL, Hackett GR, Kunkel JG, Lord EM, Hepler PK (1999) Uncoupling secretion and tip growth in lily pollen tubes: Evidence for the role of calcium in exocytosis. Plant J **19:** 379–386

Sanati Nezhad A, Geitmann A (2013) The cellular mechanics of an invasive lifestyle. J Exp Bot **64:** 4709–4728

Sanati Nezhad A, Ghanbari M, Agudelo CG, Naghavi M, Packirisamy M, Bhat RB, Geitmann A (2014) Optimization of flow assisted entrapment of pollen grains in a microfluidic platform for tip growth analysis. Biomed Microdevices **16:** 23–33

Sanati Nezhad A, Naghavi M, Packirisamy M, Bhat R, Geitmann A (2013) Quantification of cellular penetrative forces using lab-on-a-chip technology and finite element modeling. Proc Natl Acad Sci USA **110:** 8093–8098

Sanders LC, Lord EM (1989) Directed movement of latex particles in the gynoecia of three species of flowering plants. Science **243:** 1606–1608

Sanders LC, Lord EM (1992) The extracellular matrix in pollen tube growth. In E Ottaviano, MS Gorla, DL Mulcahy, and GB Mulcahy, eds, Angiosperm Pollen and Ovules. Springer New York, New York, NY, pp 238–244

Shamsudhin N, Atakan HB, Laubli N, Vogler H, Chengzhi Hu, Sebastian A, Grossniklaus U, Nelson BJ (2016) Probing the micromechanics of the fastest growing plant cell - the pollen tube. Conf Proc IEEE Eng Med Biol Soc **2016:** 461–464

Williams JH (2012) Pollen tube growth rates and the diversification of flowering plant reproductive cycles. Int J Plant Sci **173:** 649–661

Williams JH, Edwards JA, Ramsey AJ (2016) Economy, efficiency, and the evolution of pollen tube growth rates. Am J Bot **103:** 471–483

Wolters-Arts M, Lush WM, Mariani C (1998) Lipids are required for directional pollen-tube growth. Nature **392:** 818–821

Zhang J, Huang Q, Zhong S, Bleckmann A, Huang J, Guo X, Lin Q, Gu H, Dong J, Dresselhaus T, Qu L-J (2017) Sperm cells are passive cargo of the pollen tube in plant fertilization. Nat Plants **3:** 17079